

# Transition Optimization for a VTOL Tail-sitter UAV

Boyang Li, Jingxuan Sun, Weifeng Zhou, Chih-Yung Wen, Kin Huat Low, and Chih-Keng Chen

**Abstract**—This paper focuses on the transition process optimization for a vertical takeoff and landing (VTOL) tail-sitter unmanned aerial vehicle (UAV). For VTOL UAVs that can fly with either hover or cruise mode, transition refers to the intermediate phases between these two modes. This work develops a transition strategy with the trajectory optimization method. The strategy is a reference maneuver enabling the vehicle to perform transition efficiently by minimizing the cost of energy and maintaining a small change of altitude. The simplified 3-degree-of-freedom (3-DOF) longitudinal aerodynamic model is used as a dynamic constraint. The transition optimization problem is then modeled by nonlinear programming (NLP) and solved by the collocation method to obtain the reference trajectory of the pitch angle and throttle offline. Simulations with the Gazebo simulator and outdoor flight experiments are carried out with the optimized forward (hover-cruise) and backward (cruise-hover) transition solutions. The simulation and experimental results show that the optimized transition strategy enables the vehicle to finish transition with less time and change of altitude compared with that by using traditional linear transition methods.

**Index Terms**—Tail-sitter, UAV, Transition, Trajectory Optimization, Flight Experiments.

## I. INTRODUCTION

UNMANNED aerial vehicles (UAVs) have been applied to various civil fields in urban areas to contribute to the development of smart cities [1]–[3]. However, the widely available UAV configurations have their obvious shortcomings [1], [4]. For example, multi-rotor UAVs have a very limited flight range and endurance, while a large space or a long runway for takeoff and landing of high-efficiency fixed-wing UAVs are not easily available in most cities. Under such circumstance, the vertical takeoff and landing (VTOL) tail-sitter UAV is a promising platform to be applied in the urban areas [4], [5], as they can not only takeoff and land vertically in the hover mode, but also cruise efficiently in the level flight mode with extended range and endurance. It combines the advantages of both rotatory-wing and fixed-wing UAVs. The tail-sitter UAV takes off and lands on the trailing edge of its wing. Once takeoff, the entire vehicle will tilt forward and then fly like the traditional fixed-wing UAVs horizontally. Compared with other configurations of VTOL UAVs such as a tilt-rotor UAV [6], [7] and a tilt-wing UAV [8], a tail-sitter UAV has a simpler and more compact structure,

B. Li, W. Zhou, and C.Y. Wen are with Interdisciplinary Division of Aeronautical and Aviation Engineering and Department of Mechanical Engineering, The Hong Kong Polytechnic University, Kowloon, Hong Kong. E-mail: (boyang.li@connect.polyu.hk, chandler.zhou@connect.polyu.hk, cy-wen@polyu.edu.hk)

J. Sun is with Temasek Laboratories, National University of Singapore, Singapore. E-mail: (tulsunj@nus.edu.sg)

K.H. Low is with School of Mechanical and Aerospace Engineering, Nanyang Technological University, Singapore. E-mail: (mkhlow@ntu.edu.sg)

C.K. Chen is with Department of Vehicle Engineering, National Taipei University of Technology, Taipei, Taiwan. E-mail: (ckchen@ntut.edu.tw)

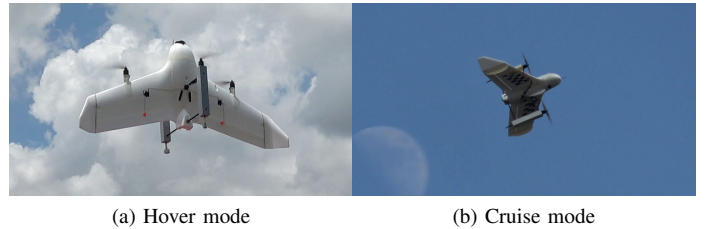


Fig. 1. Quad-rotor tail-sitter UAV prototype in different flight modes.

which reduces the use of rotation mechanism and improves the overall reliability. The tail-sitter UAV developed in this work called “PolyU-Plus Tail-sitter (PPT)” is shown in Fig. 1 with its hover and cruise state during outdoor flights.

The typical flight phases of tail-sitter VTOL UAVs include vertical takeoff, pitch down for about  $90^\circ$  into the level flight mode (forward transition), cruise flight, pitch up for about  $90^\circ$  to the hover flight mode (backward transition) and landing vertically. Transition control is one of the key challenges for all kind of VTOL aircraft, especially for tail-sitters. First of all, the traditional multi-rotor or fixed-wing controller may not be applicable in the transition period. The linearized model around trim points for either the hover or the cruise mode will be contradicted during the transition. Second, the aerodynamic forces and control efforts in the transition period are nonlinear due to the potential high angle of attack (AOA) condition. Finally, the transition period has multiple constraints to be satisfied in order to successfully enter the other flight mode. Multiple performance indexes can also be optimized, such as the change of height, the cost of energy, and transition duration.

The current available linear transition method that is used by the open source flight controller firmware PX4 (v1.8.0) [9] adopts a simple reference maneuver to make the vehicle finish transition. A linear (for forward transition) and a step (for backward transition) pitch angle commands, together with the corresponding constant throttle value during the transition are provided. These two command reference curves are set by intuition and experience, aiming to lead the vehicle to satisfy the pitch angle and airspeed requirements to finish transition. Although these linear references could guide the vehicle to finish transition, they usually leads to a large increase of altitude during transition, which is not favorable for the efficient of whole flight mission. The extra energy and time will be consumed to return to the originally planned operation altitude when transition is finished. The unpredictable change of height may also cause a safety threat to the tail-sitter UAV itself or the surrounding vehicles. In this work, we aim to develop an optimized trajectory to enable the tail-sitter UAV to finish transition with a minimum energy cost and a small

change of height.

The study of transition process began from the early stage of tail-sitter UAV development. Stone and Clarke [10], [11] firstly proposed the optimization requirements and simulation results for transition maneuver of their “T-wing” tail-sitter. They studied the influence of the vehicle’s mass and thrust-weight ratio on the transition results. Johnson *et al.* [12] discussed the use of dynamic inversion with the neural network adaption to form a single adaptive controller to control a fixed-wing UAV in all the hover, level, and transition flights. Their experimental results showed the altitude increase of about 30 m with slower and faster transitions. Frank *et al.* [13] used a pseudo-position far away from the hover position for the forward transition of a fixed-wing UAV in a constrained indoor environment. Osborne [14] tested a feedback linearization and an adaptive controller for transition trajectory tracking of a light fixed-wing UAV. Unfortunately, none of the two controllers showed good tracking performance in their experimental results.

Kita *et al.* [15] calculated a reference trajectory of the pitch angle using the relationship of the horizontal speed and the pitch angle by simulations to get the shortest time transition trajectory. However, they did not discuss the change of height during transition in detail for their experimental results. Jung and Shim [16] designed a transition controller with the L1 adaptive control and the dynamic inversion method. But the outer loop commands they used were almost linear lines from initial to the target value of transition, which usually led to a large increase of height in their simulation and experimental results. Naldi and Marconi [17] formulated minimum-time and minimum-energy optimal transition problems to compute the reference transition maneuvers. They transferred the transition problem to a reduced complexity mixer-integer nonlinear programming and solved it by a commercial software with collocation method. However, they showed only the numerical solutions of the problem, without providing simulation or experimental results with the UAV prototype.

Zhang *et al.* [18] provided a different strategy to deal with transition. Their vehicle conducted a 90-degree yaw rotation before transition and yaw back after transition to reduce the effect of disturbances caused by the wing. Forshaw *et al.* [19] studied the transition architecture for a twin rotor tail-sitter UAV and showed simulation results with the linear transition method. Banazadeh and Taymourtash [20] used the cross-coupled thrust-vectoring control to generate optimal transition trajectories for a tail-sitter UAV. They took the physical constraints into the optimization process to guarantee that the estimated trajectories are feasible. The influence of thrust-to-weight ratio to transition was analyzed.

Zhou *et al.* [21] developed a unified control framework to enable a quad-rotor tail-sitter to conduct all flight modes with a single controller. Only were simulation results showed. Oosedo *et al.* [22], [23] showed the experimental results of transition flight with two different cost functions. The improvement of their optimized controller was quite limited compared with the normal linear controller. Verling *et al.* [24] optimized the backward transition with a self-designed cost function. They showed a single-time experimental result of backward transition with a less change of altitude after optimization.

Nevertheless, the optimized transition had a height drop and increased horizontal displacement. Zhang *et al.* [25] and Li *et al.* [26] also presented simulation results of their proposed transition methods with self-designed tail-sitter UAV models.

Relevant studies about hover-cruise and cruise-hover maneuvers for aerobatic fixed-wing UAVs are also worth noting. Green and Oh [27] designed a hybrid UAV with a small propeller at each wingtip. They mainly discussed the quaternion attitude control algorithm for cruise-to-hover control. Ure and Inalhan [28] developed a multi-modal flight control and path planning scheme for the fixed-wing UAV to perform agile maneuvers with a pre-defined library. The change of flight modes was handled by dynamic sliding mode control. Bulka and Nahon [29] introduced the attitude, position, and thrust controller for an aerobatic fixed-wing UAV to conduct aggressive maneuvers such as knife-edge and hover. Based on these controllers, Levin *et al.* [30] used a numerical optimal control method to generate reference trajectories and feed-forward control inputs for automatic agile maneuvers. In the following work, Levin *et al.* [31] used the rapidly-exploring random trees (RRT) to generate the obstacle-free path for the UAV and then track the path by agile maneuvers.

Although the excellent works mentioned above with linear or optimal transition methods have been demonstrated, none of them has presented satisfactory experimental results with an obvious reduced change of height after transition. Some of them only presented one-time experimental result which is insufficient to prove the effectiveness and robustness of their proposed methods accounting to the variant disturbances of the outdoor environment. The studies about aerobatic fixed-wing UAVs focused more on the successful execution of various maneuvers rather than the detailed performance on transition. Therefore, this work is motivated to develop a tail-sitter transition optimization framework with trajectory optimization method and verify its performance by repeated experiments. A cost function was proposed to minimize the energy cost and tracking error during transition. The 3-DOF longitudinal dynamic model, boundary conditions, physical limits of states and actuators were used as the constraints. The optimal transition problem is then coded into nonlinear programming (NLP) and solved by direct collocation methods. We also introduced a quick evaluation process to implement the optimal reference into the simulation and experimental platform. The simulations and multiple flight experiments showed good improvement in transition performance with the proposed optimized transition references.

The remaining sections of this paper is organized as follows: the tail-sitter UAV prototype and dynamic model are described in Section II; Section III presents the transition optimization methods with results of both forward and backward transitions; The simulation results are given in Section IV and outdoor flight experimental results are shown in Section V. Finally, the conclusions and future work are addressed in Section VI.

## II. SYSTEM MODELING

In this section, the developed cross-type tail-sitter UAV prototype by our previous study [32], [33] is briefly described,

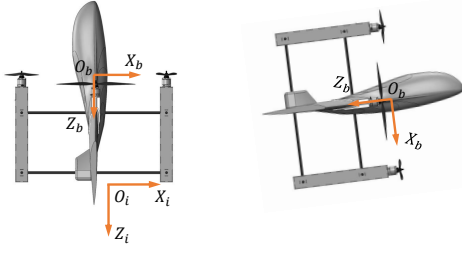


Fig. 2. Coordinates of tail-sitter UAV in hover and cruise flight mode.

followed by the introduction of coordinate systems. The simplified dynamic model and aerodynamic model are finally presented.

### A. Tail-sitter UAV Prototype Description

The tail-sitter prototype was modified from an EPO material flying-wing UAV airframe kit ‘Skywalker-X8’ with the original rear motor removed. Four added propulsion sets were fixed on the airframe forming a ‘+’ configuration similar to the quadrotor UAV. Two of them were linked to the leading edges of the left and right wings. The other two motors were mounted on wooden structures in the front and back of the wing and connected by carbon tubes. The takeoff weight of current platform is up to 2 kg with a wing span of 1.1 m. Four rotors can provide thrust and control moments in three axes similar to quad-rotor UAVs. The prototype used Pixhawk as the flight controller hardware and PX4 autopilot as the base software platform. The flexible open source flight control platform enables users to modify it according to different customize requirements.

### B. Assigned Coordinate Systems

For the tail-sitter UAV, two right-handed coordinate systems are used to describe the states of vehicle (see Fig. 2). The initial frame ( $O_i : X_i; Y_i; Z_i$ ) is fixed at the takeoff position pointing to north-west-down (NED) directions of the earth. The body frame ( $O_b : X_b; Y_b; Z_b$ ) is fixed at the center of gravity (CG) of the UAV with  $X_b$  axis pointing to the down-side of the wing and other axes following right-hand principle. The position of the vehicle in  $O_i$  is defined by  $\mathbf{p}_i = [X \ Y \ Z]^T$ , velocity in  $O_i$  is described by  $\mathbf{v}_i = [X \ Y \ Z]^T$ . The velocity of the vehicle in  $O_b$  is defined by  $\mathbf{v}_b = [U \ V \ W]^T$ . The attitude of the vehicle is described by quaternions in the simulation model and the attitude controller. For an intuitive illustration in results presentation, the quaternions are converted to Euler angles with  $\phi; \theta; \psi$  as roll, pitch, and yaw angles defined in the hovering state. It should be noted that based on the above definition, the pitch angle  $\theta = 0^\circ$  at the takeoff, landing, and hover condition. When the vehicle transition forward in the air into cruise flight, the pitch angle  $\theta = 90^\circ$ .

### C. Three-DOF Longitudinal Dynamic Model

Although transition flight is a complex nonlinear process, the significant change of states mainly happens in the vertical

plane. The other states such as roll, yaw, and side displacement only need to be stabilized at the original trim condition before transition. Longitudinal equations of motion include horizontal and vertical velocities in the body coordinate, and the rotations about the  $Y_b$ -axis, described by  $\theta$ . If we neglect the coupling relationship between the longitudinal dynamics and dynamics of other directions, we can simplify the full 6-DOF dynamic model into a 3-DOF model for the transition process study. Compared with the 6-DOF rigid body dynamic model, this 3-DOF model significantly reduced the size of the optimization problem. The difference between hover and cruise flights are mainly represented by pitch angle and airspeed. If the vertical velocity is much smaller than the horizontal velocity during transition, the horizontal velocity  $X_i$  will be the same as the airspeed, which is used as one of the criteria to mark the finish of transition. During transition, we would also like to have a minimal change of height. This requirement can be satisfied by constraining vertical speed  $Z_i$  in the model to a small value. As a result, the states  $\mathbf{x}$  for the 3-DOF dynamic model includes velocity in  $X_i, Z_i$  direction, and the pitch angle,  $\mathbf{x} = [X_i \ Z_i \ \theta]^T$ .

For our tail-sitter UAV system, PX4 Pro [34] open-source hardware and firmware has been used for the basic avionic system. This system showed stable performance in basic hover and cruise flight in our previous study [35]. It also provides plenty of interface for us to modify the original sub-modules and functions. The optimization of transition can be emphasized on either attitude control or the reference trajectory. Based on our previous flight results [36], it was found that the performance of attitude controllers provided by the PX4 firmware can satisfy the attitude control requirement during hover and transition period. In this work, we will only focus on the development of the outer-loop reference of transition maneuver, while employing the original multi-rotor and fixed-wing attitude controllers from PX4. The attitude control can be assumed as the first-order dynamic system with a time constant of  $\tau$  [37], the 3-DOF dynamic model of the tail-sitter can be written as

$$\begin{aligned} \dot{X}_i &= (F_t = m) \sin \theta + F_{\text{aero},x} = m \dot{X}_i \\ \dot{Z}_i &= 4g (F_t = m) \cos \theta + F_{\text{aero},z} = m \dot{Z}_i \\ \dot{\theta} &= \dot{\theta} \end{aligned} \quad (1)$$

where  $m$  is the mass of vehicle,  $F_t$  is the total thrust generated by the four propellers,  $\theta$  is the command pitch angle, and  $F_{\text{aero},x}, F_{\text{aero},z}$  are  $X_i$  and  $Z_i$  components of aerodynamic forces including lift  $L$  and drag  $D$ . The first two relationships are obtained from the first principle in the initial coordinate while the last relation is acquired by the 1-st order assumption to the inner attitude loop of pitch angle control.

For the dynamic model considered, the outputs of the transition optimizer are the commanded total thrust and pitch angle,  $\mathbf{u} = [F_t \ \theta]^T$ .

### D. Aerodynamic Model

The aerodynamic model should be involved in the transition model since the lift and drag will change significantly when the UAV pitches down, increases the horizontal speed, and

transits to the cruise flight in the forward transition, and vice versa. Lift and drag forces can be calculated by

$$\begin{aligned} L &= \frac{1}{2} \rho V^2 S C_L(\alpha); \\ D &= \frac{1}{2} \rho V^2 S C_D(\alpha); \end{aligned} \quad (2)$$

where  $\rho$  is the density of air,  $V$  is the airspeed,  $S$  is the wing area, and  $C_L$  and  $C_D$  are the corresponding lift and drag coefficients at the certain angle of attack  $\alpha$ , respectively. The angle of attack is defined by  $\alpha = \tan^{-1} W/U$ . The velocity in the body frame,  $U$  and  $W$ , can be calculated by the coordinate transformation of the inertial frame speeds.

For the aerodynamic model in the transition study, the experimental data of lift and drag coefficients versus angle of attack for NACA 0012 airfoil from report [38] are fitted in Fig. 3. Although the actual airfoil of our tail-sitter is not exactly the same with NACA 0012, the error is regarded as acceptable when building a model-based controller for a tail-sitter UAV [39].

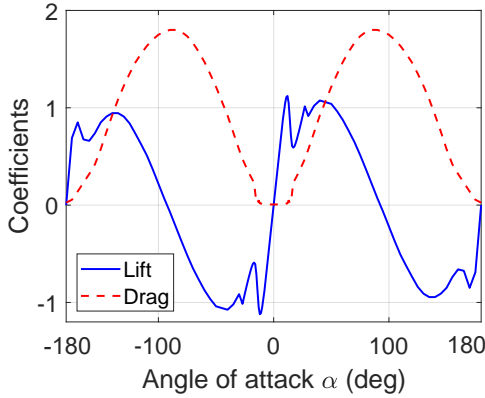


Fig. 3. Lift and drag coefficients for NACA-0012 airfoil.

### III. TRANSITION OPTIMIZATION

As the dynamic model for the transition has been built, we will then optimize this process according to certain objectives and constraints with the numerical method. The optimization results will be the throttle and pitch commands at a minimum cost while keeping a small change of height.

#### A. Transition Control Structure

During the hover flight, the weight of the vehicle is supported by the propulsion system facing up. When conducting the cruise flight, the vehicle is supported by lift generated from the wing and the propulsion system will face forward to provide thrust. The transition process is the intermediate state between these two trimmed conditions. During the transition period, the weight of the vehicle is supported by the combination of these two mechanisms. To utilize the well-developed multi-rotor and fixed-wing flight controllers, the VTOL UAVs usually adopt compound controller structures, which means all the multi-rotor, fixed-wing, and transition controllers are running simultaneously onboard during the flight. There will

be certain signal selectors to decide the source of commands that are finally received by the actuators in different flight phases. The structure and transition logic of the controller used in this tail-sitter UAV for both the linear and optimized transition methods is presented in Fig. 4.

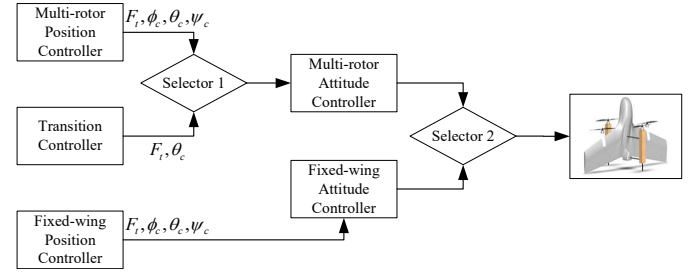


Fig. 4. Controller structure for allocating signal source during different flight modes.

During hover and cruise flight modes, the vehicle will be controlled by the cascaded position and attitude controllers for multi-rotor and fixed-wing UAV, respectively. When the forward or backward transition process is triggered, the outer-loop position controller will be replaced by a transition controller sending the commanded throttle and attitude to the multi-rotor attitude controller. When the logic selectors check that the vehicle has reached the criteria for finished transition, it will reroute the signal flow accordingly. To better describe the transition process, the quantitative definitions of both forward and backward transitions will be given first.

1) *Forward Transition*: The forward transition is a process to lead the tail-sitter UAV flying from the hover flight mode into the cruise flight mode. For the coordinate definition shown in Fig. 2, the UAV flies with pitch angle  $0^\circ$  and airspeed  $V = 0$  m/s in hover flight. While in the cruise mode, the UAV flies at  $70^\circ$  and  $V = 12$  m/s for this vehicle prototype. During the forward transition, the target final value of pitch angle and airspeed should be near the operation point of the fixed-wing mode so that the vehicle can be taken over by the fixed-wing flight controllers smoothly. The initial and final states for the forward transition are shown in Table I.

TABLE I  
THE DEFINITION OF FORWARD TRANSITION.

State	Initial Value	Final Value
Pitch Angle ( $^\circ$ )	0	< 65
Airspeed (m/s)	0	> 10

2) *Backward Transition*: The backward transition can be regarded as the reverse process of forward transition. The vehicle usually conducts backward transition before the final vertical landing stage. The initial state of backward transition is cruise flight handled by the fixed-wing flight controllers. The final state of backward transition is hovering flight mode with a small pitch angle and a low flight speed. After the backward transition, the vehicle should enter a domain where the multi-rotor flight controllers could take over. The initial and final states of backward transition are presented in Table II.

TABLE II  
THE DEFINITION OF BACKWARD TRANSITION

State	Initial Value	Final Value
Pitch Angle (°)	< 65	> 15
Airspeed (m/s)	> 12	< 5

### B. Optimization Method

In a transition process, one would like the UAV to finish transfer between two trimmed conditions in a limited time. Besides, one would also prefer to minimize or maximise some indices to improve the performance of transition. Such indices could be transition time, change of altitude, cost of energy, etc. In this work, the tail-sitter transition process is considered as a trajectory optimization problem, defined by finding an optimal control sequence  $\mathbf{u}^*(t)$  from the allowed region  $U$  to make the states transfer from initial states  $\mathbf{x}(t_0)$  to the target final states  $\mathbf{x}(t_F)$  with a minimized value of objective function along this trajectory.

The optimization problem can usually be solved by direct and indirect methods. Direct methods parameterize the infinite dimensional decision variables to a limited extent so that the problem can be approximated by a finite dimensional nonlinear programming (NLP), and then be addressed by numerical methods such as collocation [40]. The process of converting the original trajectory optimization into nonlinear parameter optimization problem is known as transcription, which means to transcribe a dynamic system into a problem with a finite set of variables. For the current tail-sitter transition, the direct method is chosen since it is easy for calculation and implementation with any offline PC or an online flight computer.

A typical formulation for nonlinear programming is shown in Eq. (3). A cost function  $J(\mathbf{u})$  is defined to measure the performance of a process with control sequence  $\mathbf{u}$ . The process should also satisfy a group of equal and unequal constraints, such as system dynamics, safety region of system states and actuator outputs.  $\mathbf{f}(\mathbf{u})$  is a group of functions representing all of the equal constraints to be satisfied and  $\mathbf{g}(\mathbf{u})$  is another group of functions representing the unequal constraints must be satisfied during the transition process.

$$\begin{aligned} & \min_{\mathbf{u}} J(\mathbf{u}) \\ \text{subject to: } & \mathbf{f}(\mathbf{u}) = \mathbf{0} \\ & \mathbf{g}(\mathbf{u}) \leq \mathbf{0}; \\ & \mathbf{u} \in U; \end{aligned} \quad (3)$$

### C. Cost Function

The cost function determines how to measure the performance of a transition when all other constraints set to complete transition are satisfied. For a general optimization problem, we would like the system to finish the process with minimal actuator efforts. We proposed a cost function with two terms (see Eq. 4). The first term is the energy cost by the propulsion system, and the second term is the aggressive level of pitch control. The energy used by the propulsion system is measured by the thrust output, and the aggressive of pitch control

is represented by the difference between the command and response pitch angles. Both of the two terms are normalized by their full range magnitude to eliminate the effect of different scales.

$$J = \int_{t_0}^{t_F} \frac{F_t(t)^2}{F_{t,\max}^2} + \frac{(\delta(t))^2}{\delta_{\max}^2} dt; \quad (4)$$

where  $t_0$  and  $t_F$  are initial and final times of transition,  $F_t(t)$  is the total thrust provided by the propulsion system during transition, which is also the main energy consumption for the vehicle.  $F_{t,\max}$  is the maximum thrust that can be provided by the propulsion system.  $\delta(t)$  and  $\delta_{\max}$  are the command and response pitch angles. The introduction of the error of command and response pitch angles aims to reduce the difference between these two values constrained by our 1-st order system assumption. The  $\delta_{\max}$  is a weight parameter introduced to adjust the importance of the second term, usually can be set from 0 to 1.

### D. Constraints

During the optimization process, multiple constraints should be satisfied to enable the vehicle to achieve transition. The first constraint is the 3-DOF dynamic model shown in Eq. 1. The other constrained parameters including time, system states, and control outputs are shown in Table III. For the time constraint,  $t_0$  is the initial time of transition which is selected as 0.  $t_F$  is the final time we would like to finish transition, which is selected as 2 s. The initial state  $\mathbf{x}_0$  and final states  $\mathbf{x}_F$  are set according to the transition requirements in Table I for forward transition. The state constrains  $\mathbf{x}(t)$  during transition are constrained according to the performance limits. For the vertical velocity  $Z_i(t)$ , it is constrained into a small region to ensure small height change during transition. The change of height is not preferred since the vehicle will need extra time or energy to resume to the originally planned cruise height. The last pair of constraints were given to the total thrust and command pitch angle.

TABLE III  
CONSTRAINED PARAMETERS FOR FORWARD TRANSITION OPTIMIZATION

Variable	Description	Constraint
$t_0$	initial time	[0;0]
$t_F$	final time	[2;2]
$X_{i0}$	initial horizontal speed	[0;0]
$Z_{i0}$	initial vertical speed	[0;0]
$\delta_0$	initial pitch angle	[0;0]
$X_{iF}$	final horizontal speed	[10;inf]
$Z_{iF}$	final vertical speed	[ -1;1]
$\delta_F$	final pitch angle	[ -90 ; 63 ]
$X_i(t)$	horizontal speed	[0;20]
$Z_i(t)$	vertical speed	[ -1;1]
$\delta(t)$	pitch angle	[ -90 ;0]
$F_t$	total thrust	[0;30]
$\delta_c$	command pitch angle	[ -90 ;0]

For backward transition optimization, the same cost function as in the forward transition was used. The corresponding

constraints for initial and final states can also be set according to Table II. The other constraints are the same as those in the forward transition.

### E. Optimization Setting and Solutions

An open source trajectory optimization software ‘OptimTraj’ [41] was selected to transcribe and solve the optimal transition problem. ‘OptimTraj’ is a MATLAB library designed to solve continuous-time trajectory optimization problems. It provides direct collocation methods for transcription and finally solves the discrete NLP with MATLAB function ‘*fmincon*’.

‘OptimTraj’ provides methods of different orders to solve the NLP problem. The Chebyshev-Lobatto orthogonal collocation method was finally chosen to solve our problem with acceptable calculation time and small oscillation for the results. The grid number of collocation points was selected as 10. The time constant of the attitude controller is selected as  $\tau = 0.1$  second, based on command and responded pitch angle data in the previous flight logs.

1) *Forward Transition*: The optimized solutions for the forward transition are shown in Fig. 5. The top two figures depict the optimized controller outputs: throttle and pitch angle command during the transition period. The bottom two figures present the simulated results of three longitudinal states by integration of the dynamic model. Clearly observed from these results, the vehicle finished transition in the transition period with all the states reached the target range of fixed-wing cruise flight. It is shown that the pitch angle requirement ( $< 65^\circ$ ) reached a bit earlier than the horizontal speed requirement ( $> 10$  m/s).

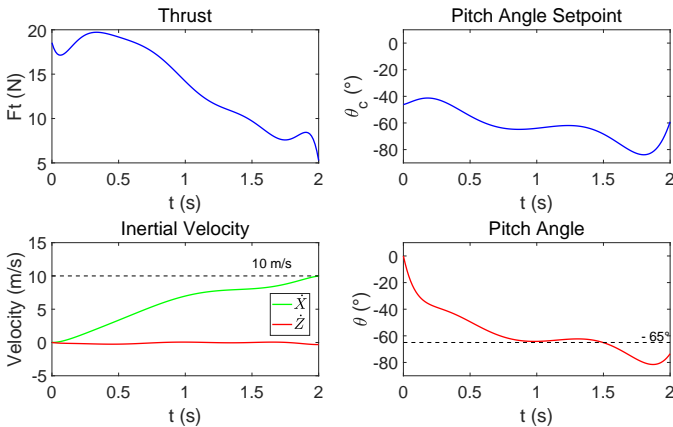


Fig. 5. Main longitudinal states of optimized solutions for forward transition. (Dashed lines show the finish criteria of forward transition)

Fig. 6 is the 2D trajectory representation of the optimized forward transition. The position is integrated by the velocity data in Fig. 5. The blue line shows the path of CG of the vehicle during transition, and the red arrow indicates the pitch attitude of the vehicle at the corresponding position. It is shown that the vehicle pitched down to cruise flight mode with a small change of altitude during the transition.

2) *Backward Transition*: The optimized backward transition results are shown in Figs. 7 and 8. As seen, the tail-sitter UAV reaches the target pitch angle at about 1.3 seconds, and

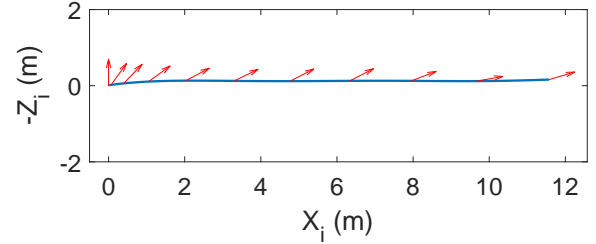


Fig. 6. 2D path and pitch angle of optimized forward transition.

then takes further time to reduce horizontal speed to switch into hover mode. The vehicle also finishes transition in 2 seconds with a nearly zero vertical speed and change of height similar to the forward transition.

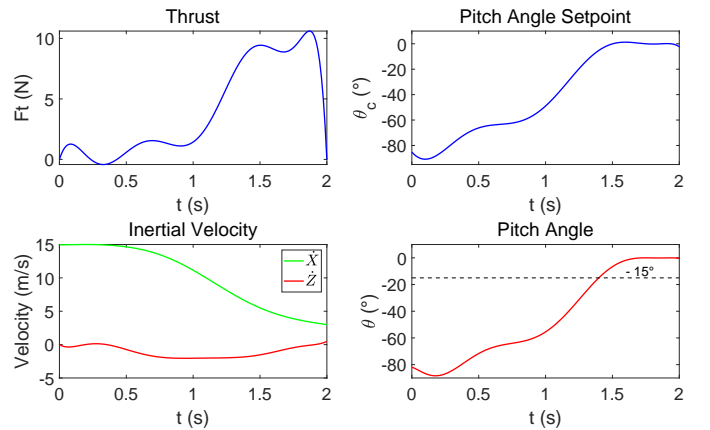


Fig. 7. Main longitudinal states of optimized solutions for backward transition. (Dashed lines show the finish criteria of backward transition)

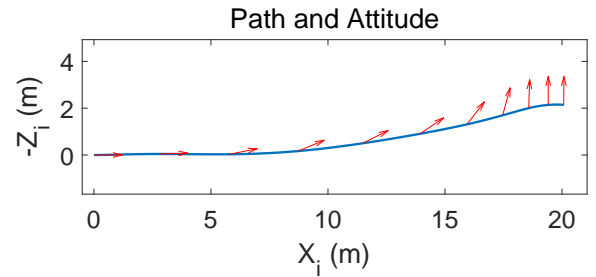


Fig. 8. 2D path and pitch angle of optimized backward transition.

## IV. SIMULATION RESULTS

### A. Simulation Environment

In this work, we first implemented and tested the optimized transition strategy in the Gazebo-PX4 software in the loop (SITL) simulation environment [42]. Gazebo has been integrated with PX4 flight control firmware, which enables the developers to simulate their algorithm with various of UAV platform including tail-sitters.

An auto-flight mission was designed to test the transition performance. The vehicle will first take off to a height of

20 m, hold there for 5 seconds, conduct forward transition, and y with the xed-wing mode for 50 m. Finally, backward transition will be conducted before landing. This action sequence was created in the ground control station software, QGroundControl, and then uploaded to the simulator. The same demonstration mission with linear and optimized transition methods for both forward and backward transition were simulated for comparison.

**B. Forward Transition Results**

1) Linear Transition Method: The linear transition method is originally provided by the PX4 open source firmware (v1.8.0). The principle of this transition strategy is to lead the vehicle to successfully transit to the other flight state by low-level control commands without considering the detailed dynamics and path of the vehicle. Generally, a simplified and practical strategy is used by focusing on the two low-level statuses - pitch angle and airspeed. To ensure safety and prevent stall, the airspeed requirement is usually preferred to be satisfied first, then followed by the pitch angle requirement. For linear forward transition, the pitch angle set-point follows a straight line connecting the current pitch angle to the target pitch angle of transition, while the throttle remains a constant value during the whole transition period. After testing with the different transition period, 2 seconds was found sufficient for the vehicle to finish transition. Therefore, only the results with transition duration of 2 seconds be shown in the following section.

The simulation results of linear transition are demonstrated in Fig. 9. The horizontal axis for each figure represents the relative time with respect to takeoff time. The vehicle is commanded with a linear decreasing pitch angle, shown with the dashed blue line in Fig. 9 (a). The solid red line shows the responded pitch angle. The throttle setpoint is a constant value of 70% for 2 seconds, shown on Fig. 9 (b). The bottom two sub-figures show the response airspeed and height of the vehicle. The shadowed area shows the transition period read from the flight log. It is found that although the vehicle can finish transition with pitch angle less than -65 and airspeed larger than 10 m/s (shown with dashed line) to enter the cruise flight mode, the altitude has increased for about 8 m.

2) Optimal Transition Method: The simulation results with the optimal transition are shown in Fig. 10. The reference thrust and pitch angle curves are fitted from the numerical solution shown in Fig. 5 by a set of 9-th order polynomials, as functions of time. The thrust was then transformed to throttle in percentage based on experimental results from [33]. The commanded pitch angle was given to the inner-loop attitude controller to follow. The commanded throttle value was provided to a 'mixer' to form the output of each motor. The results demonstrate that the vehicle can finish transition and enter the xed-wing mode with less time than the linear transition method and the change of altitude is also smaller. One of our main optimization objectives is the height reference and an open loop throttle command curve for the vehicle to track. The results of linear backward transition are shown in Fig. 11. For linear backward transition, the pitch

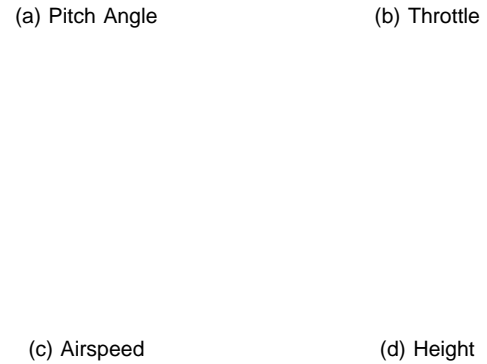


Fig. 9. Linear forward transition results by Gazebo simulation. (The shadows areas cover the transition period and dashed lines show the transition finish criterion)

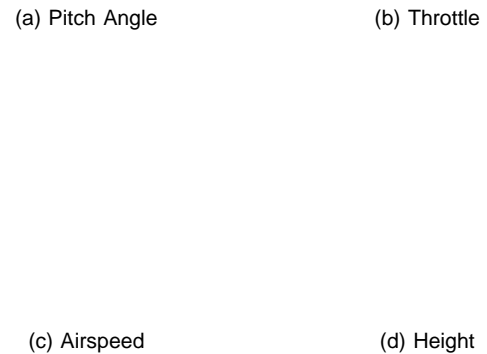


Fig. 10. Optimal forward transition result by Gazebo simulations. (The shadows areas cover the transition period and dashed lines show the transition finish criterion)

**C. Backward Transition Results**

1) Linear Transition Method: After the forward transition, two backward transition methods by the Gazebo environment were simulated. Similar to the linear forward transition, the linear back transition also aims to provide a simple pitch angle change. The optimized transition method reduces the change of height from 8 m by the linear transition method to about 4.5 m. The results of linear backward transition are shown in Fig. 11. For linear backward transition, the pitch

angle set-point follows a step curve, directly jumping to the hover point while the throttle is still a constant value similar to the linear forward transition. From the results, the vehicle is found nish backward transition in about 1.2 seconds with a height increase of about 11 m.



Fig. 11. Linear backward transition results by Gazebo simulation. (The shadows areas cover the transition period and dashed lines show the transition nish criterion)

2) Optimal Transition Method: The backward transition results with the optimal transition method are shown in Fig. 12. The vehicle is found nish backward transition in about 1.2 seconds and only climb with 6 meters after backward transition.

V. EXPERIMENTAL RESULTS

A. Experimental Environment

When the effect of optimized transition method was veri ed by the simulation environment, it was implemented directly to the Pixhawk autopilot hardware to conduct the outdoor ight experiment. The experiment aims to test the performance of the optimized transition strategy in complicated outdoor application scenarios with our tail-sitter UAV prototype. The ight tests were conducted at the ight site of Hong Kong Model Engineering Club (HKMEC), Yuen Long, Hong Kong for four days. The test times were selected with a relative calm weather status and minor wind disturbance. Totally, 11 ights and 32 transition motions were conducted with different transition methods discussed in this article. The ight data during each transition were extracted from the full ight log. Only the transition processes with the similar initial status are presented.

B. Forward Transition Results

1) Linear Transition Method: First, the original linear tran- sition method provided by the PX4 open source controller was

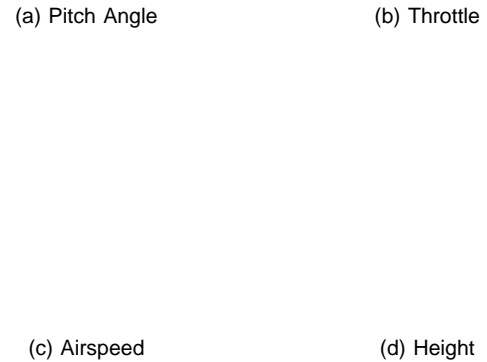


Fig. 12. Optimal backward transition result of Gazebo simulation. (The shadows areas cover the transition period and dashed lines show the transition nish criterion)

tested, with results shown in Fig. 13. Similar to the previous simulation results, the vehicle nished forward transition in about 2 seconds with the linear pitch down command and constant throttle, whereas the height increased for about 20 meters after transition.

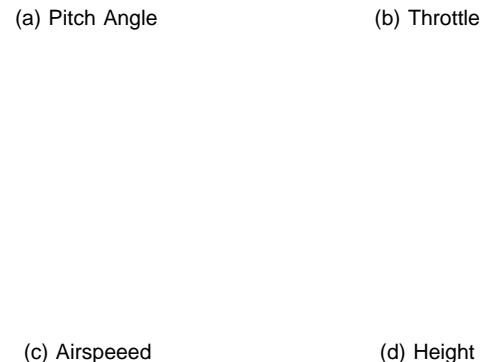


Fig. 13. Experimental result of linear forward transition. (The shadows areas cover the transition period and dashed lines show the transition nish criterion)

2) Optimal Transition Method: The results of optimized forward transition are presented in Fig. 14. With the optimized pitch angle and throttle references, the forward transition was



actually finished in about 1 second with height increased for only 2 meters.

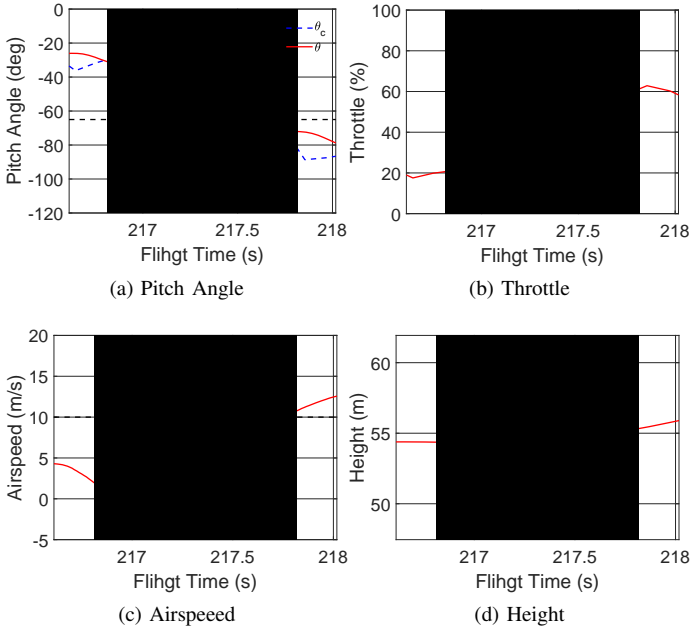


Fig. 14. Experimental result of optimal forward transition. (The shadows areas cover the transition period and dashed lines show the transition finish criterion)

3) *Comparison*: For each transition method, the flight tests were repeated for more than three times to reduce the effect of environmental disturbance. The transition duration and height change for linear and optimal forward transitions are compared in Fig. 15 and Table IV. It is noted that both the transition duration and change of height have reduced significantly after optimization.

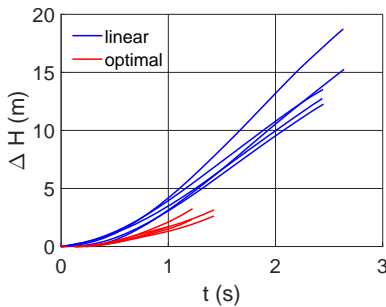


Fig. 15. The comparison of transition duration and height change of two forward transition methods for five repeated tests.

TABLE IV

COMPARISON OF AVERAGED TRANSITION TIME AND HEIGHT CHANGE FOR FIVE LINEAR AND OPTIMAL FORWARD TRANSITION TESTS.

Transition Type	Method	Average $t$ (s)	Average $H$ (m)
Forward	Linear	2.51	14.51
	Optimal	1.34	2.89

### C. Backward Transition Results

After the effectiveness of the optimized forward transition has been verified, the linear and optimal backward transition were tested.

1) *Linear Transition Method*: The experimental results of backward transition with the linear method are shown in Fig. 16. After backward transition, the vehicle gained height for about 8 m with the linear transition method. This change of height is unfavorable since the descending rate for tail-sitter cannot be too large (less than 2 m/s for our prototype). The extra gain of height will increase the time and energy consumption for landing.

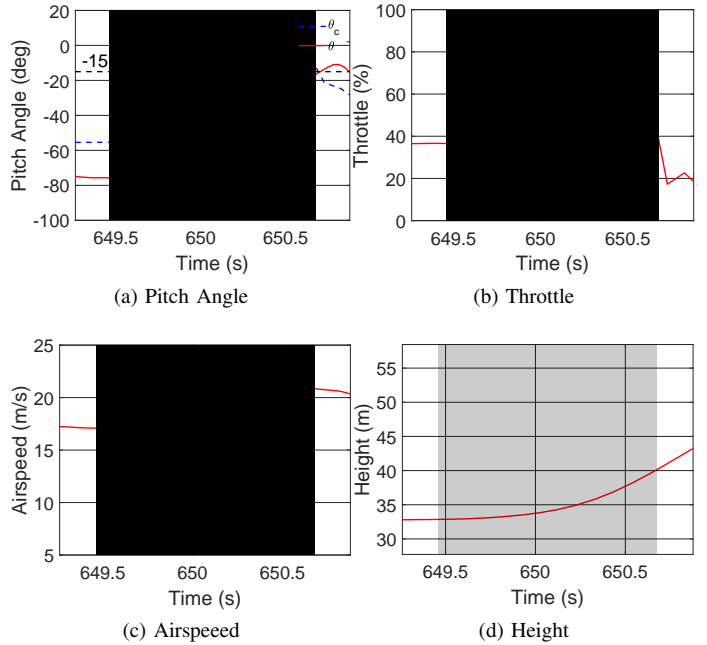


Fig. 16. Experimental result of linear backward transition. (The shadows areas cover the transition period and dashed lines show the transition finish criterion)

2) *Optimal Transition Method*: The improvement can be found in the experimental results of optimized backward transition, as shown in Fig. 17. The transition duration did not change much compared with linear transition, but the change of height has reduced from 8 m to around 4 m.

3) *Comparison*: The comparison of the experimental results of both linear and optimal backward transition methods for three corresponding repeated tests is shown in Fig. 18 and Table V. It is found that the change of height has reduced by about half with the optimized transition method. Also noticed is that the improvement for backward transition is smaller than that for forward transition. The difference is likely to be caused by the difference of dynamic response between the forward and backward transitions.

## VI. CONCLUSION

The work presented in this paper is concerned with the transition trajectory optimization for tail-sitter VTOL UAVs. The 3-DOF dynamic and aerodynamic models were developed to reflect the main characteristics of transition flight. The

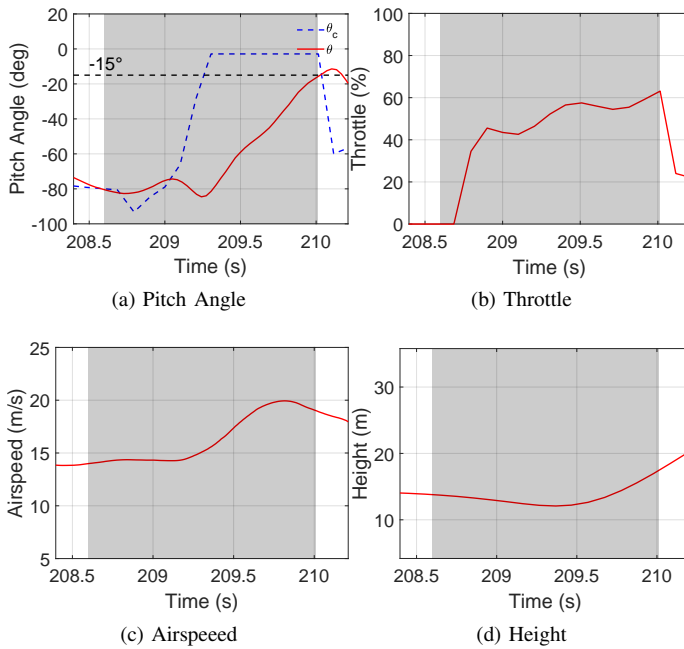


Fig. 17. Experimental result of optimal backward transition. (The shadows areas cover the transition period and dashed lines show the transition finish criterion)

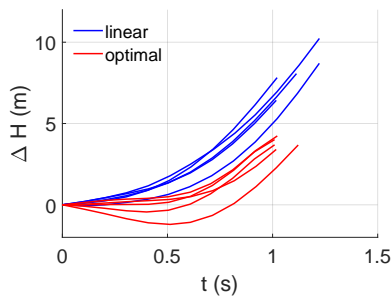


Fig. 18. The comparison of transition duration and height change of two backward transition methods for five repeated tests.

TABLE V

COMPARISON OF AVERAGED TRANSITION TIME AND HEIGHT CHANGE FOR FIVE LINEAR AND OPTIMAL BACKWARD TRANSITION TESTS.

Transition Type	Method	Average $t$ (s)	Average $H$ (m)
Backward	Linear	1.12	8.24
	Optimal	1.04	3.79

optimal transition problem was formed by a cost function to minimize the energy cost and a series of constraints. The optimal control problem was then discretized and transcribed into an NLP problem. The direct collocation method was used to get the optimized trajectory. The Gazebo robot simulator was used to verify the performance of the integrated optimized transition trajectories. Outdoor flight experiments were carried out with different transition methods. Both simulation and experimental results show that the optimized transition trajectory enabled the tail-sitter UAV to finish both forward and backward transitions with shorten duration and fewer height increment compared with the linear transition method used in

PX4 (v1.8.0). This optimization method can also be used for other tail-sitter UAVs by simply changing the vehicle parameters in the dynamic model and constrains of the optimization process. In the future, the optimization framework could be potentially implemented by combining the nonlinear model predictive control (MPC) to form a closed-loop control manner with reference paths and to provide more predictable transition results.

#### ACKNOWLEDGMENT

This work is supported by Innovation and Technology Commission, Hong Kong under Contract No. ITS/334/15FP and Research Institute for Sustainable Urban Development (RISUD) of The Hong Kong Polytechnic University.

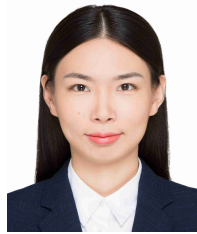
#### REFERENCES

- [1] M. Hassanalani and A. Abdelkefi, "Classifications, applications, and design challenges of drones: A review," *Progress in Aerospace Sciences*, vol. 91, pp. 99–131, May 2017.
- [2] J. Sun, B. Li, Y. Jiang, and C.-Y. Wen, "A camera-based target detection and positioning UAV system for search and rescue (SAR) purposes," *Sensors*, vol. 16, no. 11, p. 1778, Oct. 2016.
- [3] B. Li, Y. Jiang, J. Sun, L. Cai, and C.-Y. Wen, "Development and testing of a two-UAV communication relay system," *Sensors*, vol. 16, no. 10, p. 1696, Oct. 2016.
- [4] A. S. Saeed, A. B. Younes, C. Cai, and G. Cai, "A survey of hybrid unmanned aerial vehicles," *Progress in Aerospace Sciences*, vol. 98, pp. 91–105, Apr. 2018.
- [5] Y. Ke, K. Wang, and B. M. Chen, "Design and implementation of a hybrid UAV with model-based flight capabilities," *IEEE/ASME Transactions on Mechatronics*, vol. 23, no. 3, pp. 1114–1125, Jun. 2018.
- [6] T. Oktay, "Performance of minimum energy controllers on tiltrotor aircraft," *Aircraft Engineering and Aerospace Technology*, vol. 86, no. 5, pp. 361–374, Aug. 2014.
- [7] T. Oktay, "Pid based hierarchical autonomous system performance maximization of a hybrid unmanned aerial vehicle (huav)," *Anadolu University Journal of Science and Technology A - Applied Sciences and Engineering*, vol. 18, no. 2, pp. 1–1, Sep. 2017.
- [8] E. Cetinsoy, S. Dikyar, C. Hancer, K. Oner, E. Sirimoglu, M. Unel, and M. Aksit, "Design and construction of a novel quad tilt-wing UAV," *Mechatronics*, vol. 22, no. 6, pp. 723–745, Sep. 2012.
- [9] "Px4-tailsitter," Jul. 2018. [Online]. Available: [https://github.com/PX4/Firmware/blob/v1.8.0/src/modules/vtol\\_att\\_control/tailsitter.cpp](https://github.com/PX4/Firmware/blob/v1.8.0/src/modules/vtol_att_control/tailsitter.cpp)
- [10] R. H. Stone and G. Clarke, "Optimization of transition manoeuvres for a tail-sitter unmanned air vehicle (uav)," in *Australian Aerospace International Congress*, Mar. 2001.
- [11] R. Stone, "Control architecture for a tail-sitter unmanned air vehicle," in *5th Asian Control Conference*, May 2004.
- [12] E. N. Johnson, A. Wu, J. C. Neidhoefer, S. K. Kannan, and M. A. Turbe, "Flight-test results of autonomous airplane transitions between steady-level and hovering flight," *Journal of Guidance, Control, and Dynamics*, vol. 31, no. 2, pp. 358–370, Mar. 2008.
- [13] A. Frank, J. McGrew, M. Valenti, D. Levine, and J. How, "Hover, transition, and level flight control design for a single-propeller indoor airplane," in *AIAA Guidance, Navigation and Control Conference and Exhibit*, Aug. 2007.
- [14] S. R. Osborne, "Transitions between hover and level flight for a tailsitter uav," Ph.D. dissertation, Brigham Young University, Dec. 2007.
- [15] K. Kita, A. Konno, and M. Uchiyama, "Transition between level flight and hovering of a tail-sitter vertical takeoff and landing aerial robot," *Advanced Robotics*, vol. 24, no. 5-6, pp. 763–781, Jan. 2010.
- [16] Y. Jung and D. H. Shim, "Development and application of controller for transition flight of tail-sitter UAV," *Journal of Intelligent & Robotic Systems*, vol. 65, no. 1-4, pp. 137–152, Aug. 2011.
- [17] R. Naldi and L. Marconi, "Optimal transition maneuvers for a class of v/STOL aircraft," *Automatica*, vol. 47, no. 5, pp. 870–879, May 2011.
- [18] W. Zhang, Q. Quan, R. Zhang, and K.-Y. Cai, "New transition method of a ducted-fan unmanned aerial vehicle," *Journal of Aircraft*, vol. 50, no. 4, pp. 1131–1140, Jul. 2013.

- [19] J. L. Forshaw, V. J. Lappas, and P. Briggs, "Transitional control architecture and methodology for a twin rotor tailsitter," *Journal of Guidance, Control, and Dynamics*, vol. 37, no. 4, pp. 1289–1298, Jul. 2014.
- [20] A. Banazadeh and N. Taymourtash, "Optimal control of an aerial tail sitter in transition flight phases," *Journal of Aircraft*, vol. 53, no. 4, pp. 914–921, Jul. 2016.
- [21] J. Zhou, X. Lyu, Z. Li, S. Shen, and F. Zhang, "A unified control method for quadrotor tail-sitter UAVs in all flight modes: Hover, transition, and level flight," in *IEEE/RSJ International Conference on Intelligent Robots and Systems*, Sep. 2017.
- [22] A. Oosedo, S. Abiko, A. Konno, T. Koizumi, T. Furui, and M. Uchiyama, "Development of a quad rotor tail-sitter VTOL UAV without control surfaces and experimental verification," in *IEEE International Conference on Robotics and Automation*, May 2013.
- [23] A. Oosedo, S. Abiko, A. Konno, and M. Uchiyama, "Optimal transition from hovering to level-flight of a quadrotor tail-sitter UAV," *Autonomous Robots*, vol. 41, no. 5, pp. 1143–1159, Jul. 2016.
- [24] S. Verling, B. Weibel, M. Boosfeld, K. Alexis, M. Burri, and R. Siegwart, "Full attitude control of a VTOL tailsitter UAV," in *IEEE International Conference on Robotics and Automation*, May 2016.
- [25] D. Zhang, Z. Chen, L. Xi, and Y. Hu, "Transitional flight of tail-sitter unmanned aerial vehicle based on multiple-model adaptive control," *Journal of Aircraft*, vol. 55, no. 1, pp. 390–395, Jan. 2018.
- [26] Z. Li, L. Zhang, H. Liu, Z. Zuo, and C. Liu, "Nonlinear robust control of tail-sitter aircrafts in flight mode transitions," *Aerospace Science and Technology*, vol. 81, pp. 348–361, Oct. 2018.
- [27] W. Green and P. Oh, "A hybrid MAV for ingress and egress of urban environments," *IEEE Transactions on Robotics*, vol. 25, no. 2, pp. 253–263, Apr. 2009.
- [28] N. K. Ure and G. Inalhan, "Autonomous control of unmanned combat air vehicles: Design of a multimodal control and flight planning framework for agile maneuvering," *IEEE Control Systems*, vol. 32, no. 5, pp. 74–95, Oct. 2012.
- [29] E. Bulka and M. Nahon, "Automatic control for aerobatic maneuvering of agile fixed-wing UAVs," *Journal of Intelligent & Robotic Systems*, vol. 93, no. 1–2, pp. 85–100, Feb. 2018.
- [30] J. M. Levin, M. Nahon, and A. A. Paranjape, "Real-time motion planning with a fixed-wing UAV using an agile maneuver space," *Autonomous Robots*, vol. 43, no. 8, pp. 2111–2130, May 2019.
- [31] J. M. Levin, A. A. Paranjape, and M. Nahon, "Agile maneuvering with a small fixed-wing unmanned aerial vehicle," *Robotics and Autonomous Systems*, vol. 116, pp. 148–161, Jun. 2019.
- [32] B. Li, W. Zhou, J. Sun, C. Wen, and C. Chen, "Model predictive control for path tracking of a vtol tailsitter uav in a hil simulation environment," in *AAA Modeling and Simulation Technologies Conference*, Jan. 2018.
- [33] B. Li, W. Zhou, J. Sun, C.-Y. Wen, and C.-K. Chen, "Development of model predictive controller for a tail-sitter VTOL UAV in hover flight," *Sensors*, vol. 18, no. 9, p. 2859, Aug. 2018.
- [34] "Px4 pro," Dec. 2018. [Online]. Available: <http://px4.io/>
- [35] J. Sun, B. Li, C.-Y. Wen, and C.-K. Chen, "Design and implementation of a real-time hardware-in-the-loop testing platform for a dual-rotor tail-sitter unmanned aerial vehicle," *Mechatronics*, vol. 56, pp. 1–15, Dec. 2018.
- [36] B. Li, "Model predictive hover control and transition optimization for a tail-sitter unmanned aerial vehicle," Ph.D. dissertation, The Hong Kong Polytechnic University, 2018. [Online]. Available: <http://hdl.handle.net/10397/80315>
- [37] M. Kamel, M. Burri, and R. Siegwart, "Linear vs nonlinear MPC for trajectory tracking applied to rotary wing micro aerial vehicles," *IFAC-PapersOnLine*, vol. 50, no. 1, pp. 3463–3469, Jul. 2017.
- [38] C. C. Critzos, H. H. Heyson, and J. Boswinkle, Robert W., "Aerodynamic characteristics of naca 0012 airfoil section at angles of attack from 0 degrees to 180 degrees," National Advisory Committee for Aeronautics Collection, resreport NACA-TN-3361, Jan. 1955. [Online]. Available: <http://hdl.handle.net/2060/19930084501>
- [39] J. Sun, "Wind-resistant hover control and wind field estimation of a vtol tail-sitter uav," Ph.D. dissertation, The Hong Kong Polytechnic University, 2018. [Online]. Available: <http://hdl.handle.net/10397/79539>
- [40] J. T. Betts, "Survey of numerical methods for trajectory optimization," *Journal of Guidance, Control, and Dynamics*, vol. 21, no. 2, pp. 193–207, Mar. 1998.
- [41] M. Kelly, "An introduction to trajectory optimization: How to do your own direct collocation," *SIAM Review*, vol. 59, no. 4, pp. 849–904, Jan. 2017.
- [42] "Gazebo simulation," Jan. 2019. [Online]. Available: <http://dev.px4.io/en/simulation/gazebo.html>



mization, and field experiments of UAS and mobile robots.



**Boyang Li** received his B.Eng. and M.Eng. degrees in Aeronautical Engineering from Northwestern Polytechnical University, Xi'an, China in 2012 and 2015, respectively. He then received the Ph.D. degree in Mechanical Engineering from The Hong Kong Polytechnic University in 2019. He was at Air Traffic Management Research Institute (ATMRI) at Nanyang Technological University, Singapore before the current position as Research Associate at the University of Edinburgh, UK. His research interests include model predictive control, trajectory optimization, and field experiments of UAS and mobile robots.

**Jingxuan Sun** received her B.S. degree in Mechanical Engineering and Automation from Xi'an University of Technology, Xi'an, China, in 2012 and her M.S. and Ph.D. degree in Mechanical Engineering from The Hong Kong Polytechnic University, Hong Kong, in 2014 and 2018, respectively. She is currently a Research Scientist in Temasek Laboratories at National University of Singapore, Singapore. Her research topics include aerial vehicle dynamics and simulation, wind field estimation, and tail-sitter VTOL UAV control.



**Weifeng Zhou** received his B.Eng. degree in Mechanical Engineering from University of Warwick, Coventry, UK, in 2015 and M.Eng. degree in Mechanical Engineering from the University of Toronto, Ontario, Canada in 2016. He is currently a Ph.D. candidate in The Hong Kong Polytechnic University, Hong Kong, focusing on tail-sitter VTOL UAV control by MPC method.



by plasma actuators on a delta wing; UAVs and MAVs; and ice accretion.

**Chih-Yung Wen** received his B.S. degree from the Department of Mechanical Engineering at National Taiwan University in 1986 and his M.S. and Ph.D. degrees from the Department of Aeronautics at the California Institute of Technology (Caltech) in 1989 and 1994, respectively. In 2012, Professor Wen joined the Department of Mechanical Engineering, The Hong Kong Polytechnic University, as a professor. His current research interests include hypersonic aero-thermodynamics; shock/droplet and shock/bubble interactions; detonation; flow control



of robotics, biomimetics, rehabilitation, UAV, air traffic management, impacts, power transmission systems, structural dynamics, and vibrations.

**Kin Huat Low** is currently a professor in the School of Mechanical and Aerospace Engineering, Nanyang Technological University (NTU) in Singapore. He obtained his BSc degree from the National Cheng Kung University in Taiwan, MSc and PhD degrees in Mechanical Engineering from the University of Waterloo, Canada. Kin Huat is leading the UAS (Unmanned Aircraft Systems) program in the ATMRI, NTU, focusing on UAS Traffic Management (UTM) and Urban Air Mobility (UAM). He has published about 330 journal and conference papers in the areas

**Chih-Keng Chen** received his B.S. and M.S. degrees in Mechanical Engineering from National Cheng-Kung University, Taiwan, in 1986 and 1988, respectively, and his Ph.D. in Systems and Control Engineering from Case Western Reserve University in Cleveland, Ohio, U.S. in 1993. He is currently a Professor with the Department of Vehicle Engineering, National Taipei University of Technology, Taipei, Taiwan. His current research interests include hydraulic systems, vehicle dynamics and control, and vehicle braking control systems.